



# Antineuroinflammatory Effects of 7,3',4'-Trihydroxyisoflavone in Lipopolysaccharide-Stimulated BV2 Microglial Cells through MAPK and NF- $\kappa$ B Signaling Suppression

Seon-Kyung Kim<sup>†</sup>, Yong-Hyun Ko<sup>†</sup>, Youyoung Lee, Seok-Yong Lee and Choon-Gon Jang\*

Department of Pharmacology, School of Pharmacy, Sungkyunkwan University, Suwon 16419, Republic of Korea

## Abstract

Neuroinflammation—a common pathological feature of neurodegenerative disorders such as Alzheimer's disease—is mediated by microglial activation. Thus, inhibiting microglial activation is vital for treating various neurological disorders. 7,3',4'-Trihydroxyisoflavone (THIF)—a secondary metabolite of the soybean compound daidzein—possesses antioxidant and anticancer properties. However, the effects of 7,3',4'-THIF on microglial activation have not been explored. In this study, antineuroinflammatory effects of 7,3',4'-THIF in lipopolysaccharide (LPS)-stimulated BV2 microglial cells were examined. 7,3',4'-THIF significantly suppressed the production of the proinflammatory mediators nitric oxide (NO), inducible nitric oxide synthase (iNOS), and cyclooxygenase-2 (COX-2) as well as of the proinflammatory cytokine interleukin-6 (IL-6) in LPS-stimulated BV2 microglial cells. Moreover, 7,3',4'-THIF markedly inhibited reactive oxygen species (ROS) generation. Western blotting revealed that 7,3',4'-THIF diminished LPS-induced phosphorylation of extracellular signal-regulated kinase (ERK), c-Jun N-terminal kinase (JNK), glycogen synthase kinase-3 $\beta$  (GSK-3 $\beta$ ), and nuclear factor kappa B (NF- $\kappa$ B). Overall, 7,3',4'-THIF exerts antineuroinflammatory effects against LPS-induced microglial activation by suppressing mitogen-activated protein kinase (MAPK) and NF- $\kappa$ B signaling, ultimately reducing proinflammatory responses. Therefore, these antineuroinflammatory effects of 7,3',4'-THIF suggest its potential as a therapeutic agent for neurodegenerative disorders.

**Key Words:** 7,3',4'-Trihydroxyisoflavone, Neuroinflammation, BV2 microglial cells, Lipopolysaccharide, Mitogen-activated protein kinase, Nuclear factor kappa B

## INTRODUCTION

As the resident innate immune cells of the central nervous system (CNS), microglia regulate inflammatory response and restore CNS homeostasis by removing pathogens and exogenous agents, such as lipopolysaccharide (LPS) (Park *et al.*, 2015). However, over-activation of microglia generates excessive proinflammatory mediators and cytokines, which lead to neurotoxicity (Kang *et al.*, 2013). For instance, neuroinflammation contributes to the pathogenesis of neurodegenerative disorders such as Alzheimer's disease, Parkinson's disease, and multiple sclerosis (Villa *et al.*, 2016; Ko *et al.*, 2019a). Therefore, controlling microglial activation by suppressing the expression of proinflammatory factors such as nitric oxide (NO) and interleukin-6 (IL-6) might be a key therapeutic strategy for neurodegenerative diseases.

In neurotoxicological and immunological research, BV2

microglial cells have been widely used as a substitute for primary microglia (Li *et al.*, 2016). LPS, a major cell wall component of gram-negative bacteria, stimulates microglia and promotes reactive oxygen species (ROS) generation (Pandur *et al.*, 2018). ROS modify the gene expression of proinflammatory mediators by altering mitogen-activated protein kinase (MAPK) cascades and activating nuclear factor kappa B (NF- $\kappa$ B) transcription factors (Park *et al.*, 2015). Activated NF- $\kappa$ B translocates to the nucleus and triggers inflammatory defense responses by modulating the release of inducible nitric oxide synthase (iNOS) and cyclooxygenase-2 (COX-2) as well as the activation of MAPK components including extracellular signal-regulated kinase 1/2 (ERK 1/2), p38 MAPK, and c-Jun NH2-terminal kinase (JNK) (Henn *et al.*, 2009).

Soybean, which is commonly consumed in traditional Asian diets, has been widely studied for its beneficial effects on the prevention of breast cancer, heart disease, and demen-

**Open Access** <https://doi.org/10.4062/biomolther.2020.093>

This is an Open Access article distributed under the terms of the Creative Commons Attribution Non-Commercial License (<http://creativecommons.org/licenses/by-nc/4.0/>) which permits unrestricted non-commercial use, distribution, and reproduction in any medium, provided the original work is properly cited.

Received May 25, 2020 Revised Jul 9, 2020 Accepted Jul 24, 2020

Published Online Aug 19, 2020

\*Corresponding Author

E-mail: jang@skku.edu

Tel: +82-31-290-7780, Fax: +82-31-292-8800

<sup>†</sup>The first two authors contributed equally to this work.

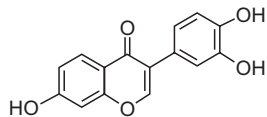


**Fig. 1.** Chemical structure of 7,3',4'-THIF.

tia (Lammersfeld *et al.*, 2009; Miguez *et al.*, 2012; Lu *et al.*, 2018). In particular, daidzein, which accounts for more than 0.1% (w/w) of the dry weight of soybeans, is one of the best understood soy isoflavones. After consumption of a soy-rich diet in humans, daidzein is further metabolized by cytochrome P450 enzymes in the liver, forming several oxidative metabolites of daidzein (Kulling *et al.*, 2001). No attempt has been made to quantitate the oxidative metabolites in humans who ingested soy products, but the three major oxidative daidzein metabolites detected were 7,3',4'-trihydroxyisoflavone (7,3',4'-THIF) (chemical structure shown in Fig. 1), 7,8,4'-THIF, and 6,7,4'-THIF (Roh, 2014). Also, these metabolites could be isolated directly from fermented soybean foods, such as natto, soy sauces, and doenjang (Korean fermented soybean paste), or microbial fermentation broth feeding with soybean meal (Chang, 2014). These daidzein metabolites also show antioxidant and anticancer activities (Rufer and Kulling, 2006; Lim *et al.*, 2017). Our previous studies have demonstrated *in vitro* antineurotoxic effects as well as *in vivo* memory-enhancing effects of 7,8,4'-THIF and 6,7,4'-THIF (Ko *et al.*, 2018, 2019a). These findings indicated that the daidzein metabolites may show neuroprotective abilities. Further research into the molecular mechanism underlying this activity is required to develop novel therapeutic targets for neurological disorders. In addition, a recent study of 7,8,4'-THIF has reported its antineuroinflammatory properties in microglia through attenuation of the Akt/NF- $\kappa$ B pathway (Wu *et al.*, 2018). Especially, 7,3',4'-THIF known to exhibit antioxidant and anti-allergenic activity, which the ortho-dihydroxy groups in these compounds play a key role for this physiological activity (Klus and Barz, 1995). However, the effects of 7,3',4'-THIF, another daidzein metabolite, on inflammation in BV2 microglial cells have not been evaluated. We hypothesized that 7,3',4'-THIF inhibits LPS-induced inflammatory responses.

This study aimed to identify the potential antineuroinflammatory effects of 7,3',4'-THIF on LPS-induced microglial activation and to explore the possible underlying mechanisms by measuring iNOS, COX-2, IL-6, and ROS production. Furthermore, the antineuroinflammatory properties of 7,3',4'-THIF were evaluated by assessing MAPK and GSK-3 $\beta$  signaling activation.

## MATERIALS AND METHODS

### Chemicals and reagents

7,3',4'-THIF was obtained from Indofine Chemical Company, Inc (San Mateo, CA, USA). The purity of 7,3',4'-THIF was >98.1%. Dimethyl sulfoxide (DMSO), 3-(4,5-dimethyl thiazol-2-yl)-2,5-diphenyl tetrazolium bromide (MTT), and lipopolysaccharide (LPS) (*Escherichia coli*, 026:B6) were purchased from Sigma Chemical Co (St. Louis, MO, USA). Dulbecco's modified Eagle's medium (DMEM) was purchased from Hyclone (Logan, UT, USA). Fetal bovine serum (FBS),

0.25% trypsin-EDTA, and penicillin/streptomycin were obtained from GIBCO-BRL (Grand Island, NY, USA). Dulbecco's phosphate-buffered saline (D-PBS) was obtained from Welgene (Gyeongsan, Korea). Anti- $\beta$ -actin antibodies were purchased from Santa Cruz Biotechnology, Inc (Dallas, TX, USA). Other primary antibodies were purchased from Cell Signaling Technology (Boston, MA, USA). Secondary antibodies were purchased from Jackson ImmunoResearch Laboratories, Inc (West Grove, PA, USA). All other chemicals were of analytical grade and were purchased from Sigma Chemical Co.

### Cell culture and treatment

BV-2 microglial cells (catalog number: CRL-2469) were obtained from ATCC (Manassas, VA, USA). BV-2 microglial cells were maintained in DMEM supplemented with 10% heat-inactivated FBS (v/v) and 0.1% penicillin/streptomycin (v/v) in a humidified atmosphere of 5% CO<sub>2</sub> and 95% air at 37°C. When the cells reached 80-90% confluency in 100-mm<sup>2</sup> cell culture dishes, they were dissociated with trypsin-EDTA and sub-cultured in culture dishes. LPS was prepared immediately before use as a 100  $\mu$ g/ml stock and diluted in PBS to the indicated final concentration. 7,3',4'-THIF was dissolved in DMSO and the stock solutions were added directly to the culture medium. In all experiments, cells were treated with the indicated concentrations of 7,3',4'-THIF in serum-free DMEM with or without LPS (100 ng/mL) and control cells were treated with DMSO alone. The final concentration of solvent was always <0.1% (v/v).

### Cell viability assay

BV2 microglial cells ( $2.5 \times 10^5$  cells/well in 24-well plates) were treated with vehicle (0.1% v/v DMSO) or 7,3',4'-THIF (10, 25, or 50  $\mu$ M) with or without LPS (100 ng/mL) treatment and incubated at 37°C in a 5% CO<sub>2</sub> incubator. Cell viability was determined 24 h later by treating with the MTT solution (5 mg/mL) for 2 h. Blue formazan crystals are formed due to the action of mitochondrial dehydrogenases in viable cells on MTT. The samples were dissolved in DMSO, and absorbance was measured at 540 nm using a microplate reader (SpectraMax 250, Molecular Device, Sunnyvale, CA, USA). Results are presented as the percentage of metabolized MTT relative to that of controls, as determined by absorbance measurements.

### Determination of NO production

BV2 microglial cells ( $2.5 \times 10^5$  cells/well in 24-well plates) were stimulated with vehicle (0.1% v/v DMSO) or 7,3',4'-THIF (10, 25, or 50  $\mu$ M) for 30 min before (pretreatment) or after (posttreatment) treatment with LPS (100 ng/mL). Culture supernatant was collected 24 h later, and nitrite concentration was determined by mixing 100  $\mu$ L of culture medium with an equal volume of Griess reagent [0.1% N-(1-naphthyl)-ethylenediamine dihydrochloride and 1% sulfanilamide in 5% phosphoric acid] in a 96-well plate. Nitrite concentration was calculated using the standard solution of sodium nitrite diluted in cell culture medium. Absorbance of each well was measured at 540 nm using a microplate reader (SpectraMax M2, San Jose, CA, USA).

### Enzyme-linked immunosorbent assay (ELISA)

BV2 microglial cells were seeded at a density of  $5 \times 10^5$  cells/well in 6-well plates and incubated overnight. After pre-

treatment with 7,3',4'-THIF (10, 25, or 50  $\mu\text{M}$ ) or vehicle (0.1% v/v DMSO) for 30 min, the cells were incubated with LPS (100 ng/mL) for 6 h. IL-6 concentration in the culture medium was determined using an IL-6 ELISA kit (Elabscience Biotechnology Co., Ltd, Wuhan, China) according to the manufacturer's instructions.

### Measurement of intracellular ROS production

Intracellular ROS production was assessed using the DCFH-DA kit (Abcam plc, Cambridge, UK) following the manufacturer's protocol. In brief, BV2 microglial cells ( $2.5 \times 10^4$  cells/well in 96-well black plates) were stained with the DCFH-DA solution (20  $\mu\text{M}$ ) at 37°C for 45 min in the dark. The cells were rinsed with wash buffer. Vehicle (0.1% v/v DMSO) or 7,3',4'-THIF (10, 25, or 50  $\mu\text{M}$ ) was added 30 min before LPS activation. After a 6-h incubation at 37°C, absorbance of each well was determined at Ex/Em=485/535 nm in the end-point mode using a microplate reader (SpectraMax M2). DCFH-DA fluorescent images were captured with a fluorescence microscope (20 $\times$  magnification).

### Western blot analysis

Western blotting was performed as previously described (Ko *et al.*, 2019b). BV2 microglial cells were seeded at a density of  $5 \times 10^5$  cells/well in 6-well plates. After pretreatment with 7,3',4'-THIF for 30 min, the cells were incubated with LPS at 37°C for 1 or 24 h. The cells were harvested by scraping with 200  $\mu\text{L}$  of ice-cold T-PER tissue protein extraction buffer (Thermo Scientific, Rockford, IL, USA) containing a phosphatase inhibitor and a protease inhibitor cocktail (Roche Diagnostics GmbH, Mannheim, Germany). After incubating on ice for 30 min, the cells were centrifuged at 10,000  $\times g$  for 15 min. The supernatant was isolated and stored at -70°C. Protein concentration was quantified using a protein assay kit (Thermo Scientific). The protein samples were separated by 8%-10% sodium dodecyl sulfate-polyacrylamide gel electrophoresis and then transferred onto polyvinylidene difluoride membranes (Merck KGaA, Darmstadt, Germany) using transfer buffer (25 mM Tris-HCl buffer, pH 7.4, containing 192 mM glycine and 20% v/v methanol). The membranes were blocked with 5% non-fat milk in 0.5 mM Tris-HCl (pH 7.5) con-

taining 150 mM NaCl and 0.1% Tween 20 for 1 h at room temperature. Each membrane was incubated with the following primary antibodies overnight at 4°C: anti- $\beta$ -actin (1:1,000), anti-iNOS (1:1,000), anti-COX-2 (1:1,000), anti-phospho JNK (1:1,000), anti-JNK (Thr183/Tyr185) (1:1,000), anti-phospho ERK 1/2 (Thr202/Tyr204) (1:2,000), anti-ERK 1/2 (1:2,000), anti-phospho GSK-3 $\beta$  (1:1,000), anti-GSK-3 $\beta$  (1:1,000), anti-phospho NF- $\kappa$ B (1:2,000), and anti-NF- $\kappa$ B (1:2,000). After washing with Tris-buffered saline with 0.1% Tween 20, the membranes were incubated in horseradish peroxidase-conjugated secondary antibodies (Jackson ImmunoResearch Laboratories, Inc) for 1 h at room temperature. Band density was determined using enhanced chemiluminescence by immersing the probed membrane in a 1:1 mixture of reagents A and B (Donginbiotech Co., Ltd, Seoul, Korea) for 5 min. The membranes were then exposed to photographic film for several minutes. Protein band intensities were calculated using densitometric analysis with ImageJ (National Institutes of Health, Bethesda, MD, USA).

### Statistics

All results were analyzed using Prism 6.0 (GraphPad Software, Inc., San Diego, CA, USA) and are expressed as mean  $\pm$  SEM. Statistical analyses were performed using one-way analysis of variance, followed by either the Newman-Keuls *post hoc* test for western blotting or Bonferroni's *post hoc* test for the others. Statistical significance was set at  $p < 0.05$ .

## RESULTS

### Effects of 7,3',4'-THIF on cell viability and LPS-induced NO production in BV2 microglial cells

To examine whether 7,3',4'-THIF is neurotoxic, the MTT assay was conducted in BV2 microglial cells with or without LPS stimulation. 7,3',4'-THIF demonstrated no neurotoxicity at any concentration (10, 25, or 50  $\mu\text{M}$ ) used in this study (Fig. 2A, 2B). Therefore, these concentrations of 7,3',4'-THIF were used in subsequent experiments.

To assess the antineuroinflammatory effects of 7,3',4'-THIF in LPS-stimulated BV2 microglial cells, NO concentration was

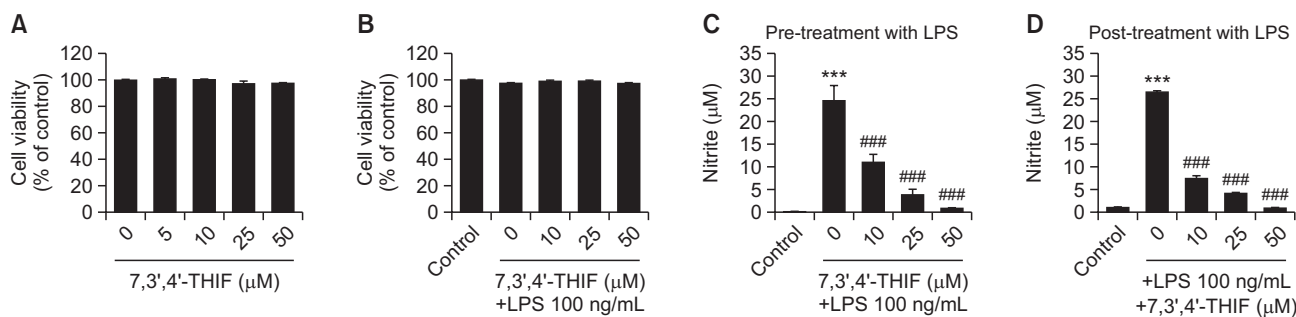


**Fig. 2.** Effects of 7,3',4'-THIF on the viability of BV2 microglial cells (A). Cells were treated with the indicated concentrations of 7,3',4'-THIF (5, 10, 25, or 50  $\mu\text{M}$ ) for 24 h. Effects of 7,3',4'-THIF on LPS-induced death of BV2 microglial cells (B). Cell viability was measured using the MTT assay and expressed as a percentage of the corresponding value of control cells. Cells were pretreated with the indicated concentrations of 7,3',4'-THIF (10, 25, or 50  $\mu\text{M}$ ) for 30 min and then activated with 100 ng/mL LPS for 24 h. Effects of 7,3',4'-THIF on LPS-induced NO release in BV2 microglial cells. Cells were pretreated (C) or post-treated (D) with the indicated concentrations of 7,3',4'-THIF (10, 25, or 50  $\mu\text{M}$ ) for 30 min and then activated with 100 ng/mL LPS for 24 h. Nitrite concentrations in the culture medium were then determined using the Griess reagent. Data are expressed as the mean  $\pm$  SEM ( $n=4-6$ ). \*\*\* $p < 0.001$  compared with the control group. ### $p < 0.001$  compared with the LPS-treated group.

measured using the Griess reagent. LPS challenge significantly increased NO concentration by almost 25  $\mu\text{M}$  compared with the control values ( $p < 0.001$  and  $p < 0.001$ , respectively) (Fig. 2C, 2D). However, the increased NO production was

significantly inhibited by 7,3',4'-THIF at all concentrations (10, 25, and 50  $\mu\text{M}$ ) during pretreatment ( $p < 0.001$ ,  $p < 0.001$ , and  $p < 0.001$ , respectively) (Fig. 2C) and posttreatment ( $p < 0.001$ ,  $p < 0.001$ , and  $p < 0.001$ , respectively) (Fig. 2D). These data show that 7,3',4'-THIF inhibits LPS-induced NO production in BV2 microglial cells.

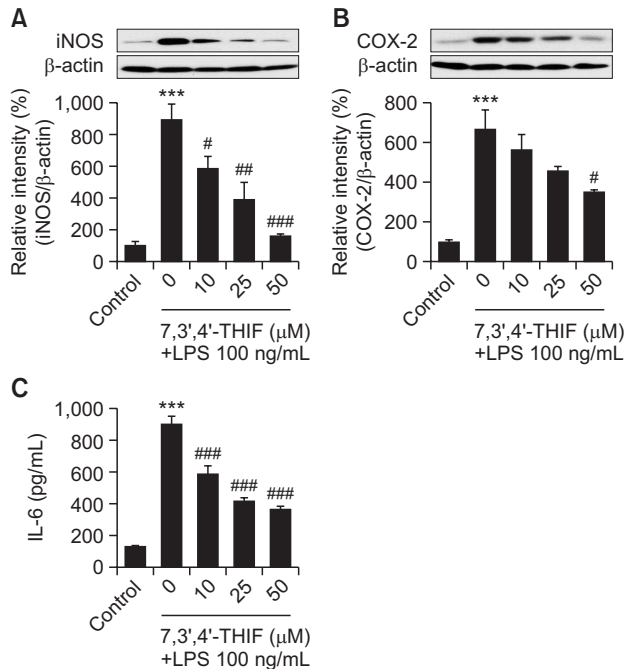


**Fig. 3.** Effects of 7,3',4'-THIF on LPS-induced upregulation of iNOS (A) and COX-2 (B) levels in BV2 microglial cells. Cells were pretreated with the indicated concentrations of 7,3',4'-THIF (10, 25, or 50  $\mu\text{M}$ ) for 30 min and then activated with 100 ng/mL LPS for 24 h. Expression levels of iNOS, COX-2, and  $\beta$ -actin were determined by western blotting. Effects of 7,3',4'-THIF on LPS-induced production of IL-6 (C) levels in BV2 microglial cells. Cells were pretreated with the indicated concentrations of 7,3',4'-THIF (10, 25, or 50  $\mu\text{M}$ ) for 30 min and then activated with 100 ng/mL LPS for 24 h. IL-6 concentrations in the culture medium were measured using commercial ELISA kits. Data are expressed as the mean  $\pm$  SEM ( $n=3-6$ ). \*\*\* $p < 0.001$  compared with the control group. # $p < 0.05$ , ## $p < 0.01$ , and ### $p < 0.001$  compared with the LPS-treated group.

**Effects of 7,3',4'-THIF on LPS-induced upregulation of iNOS, COX-2, and IL-6 in BV2 microglial cells**

LPS treatment activates iNOS in microglia, resulting in increased production of NO. LPS also induces COX-2 overexpression, which mediates prostaglandin and inflammatory cytokine synthesis (Kim *et al.*, 2014). Therefore, we assessed iNOS and COX-2 expression in microglia using western blotting. Our results showed that LPS challenge significantly increased iNOS and COX-2 levels up to 893.7% ( $p < 0.001$ ) (Fig. 3A) and 664.8% ( $p < 0.001$ ) (Fig. 3B) of the control values. However, 10 and 25  $\mu\text{M}$  7,3',4'-THIF effectively decreased iNOS levels to 586.3% ( $p < 0.05$ ) (Fig. 3A) and 392.7% ( $p < 0.01$ ) of the control values in LPS-stimulated BV2 microglial cells. Moreover, pretreatment of BV2 cells with 50  $\mu\text{M}$  7,3',4'-THIF dramatically mitigated the increased iNOS and COX-2 levels to 164.0% ( $p < 0.001$ ) (Fig. 3A) and 347.7% ( $p < 0.05$ ) of the control values in response to LPS.

To examine the effects of 7,3',4'-THIF on proinflammatory cytokine production, we measured IL-6 release using ELISA. LPS-stimulated BV2 cells showed significantly increased IL-6 production to 671.3% of the control value ( $p < 0.001$ ) (Fig. 3C). Moreover, 7,3',4'-THIF inhibited IL-6 production in a concentration-dependent manner (10, 25, or 50  $\mu\text{M}$ ) ( $p < 0.001$ ,  $p < 0.001$ , and  $p < 0.001$ , respectively) (Fig. 3C). These results suggest that 7,3',4'-THIF exerts antineuroinflammatory effects by modulating inflammatory mediators.

**Effects of 7,3',4'-THIF on LPS-induced ROS accumulation in BV2 microglial cells**

LPS-induced ROS accumulation promotes neuronal cell death and promotes excessive inflammatory responses (Cui *et al.*, 2015). Therefore, we next investigated the effects of 7,3',4'-THIF on LPS-induced intracellular ROS generation using DCFH-DA, a fluorogenic dye that measures ROS activity. Cells treated with LPS exhibited markedly increased in-

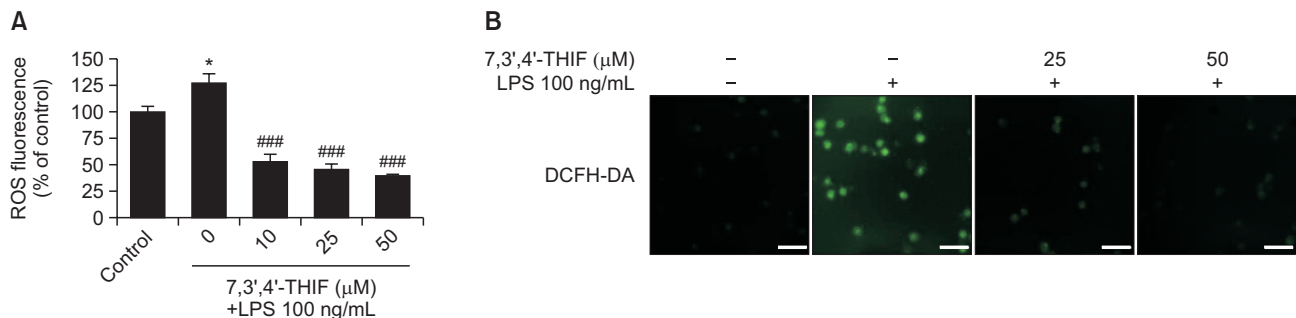


**Fig. 4.** Effects of 7,3',4'-THIF on LPS-induced ROS production (A) in BV2 microglial cells. Cells were pretreated with the indicated concentrations of 7,3',4'-THIF (10, 25, or 50  $\mu\text{M}$ ) for 30 min and then activated with 100 ng/mL LPS for 24 h. ROS levels were measured using commercial ROS kits (Abcam plc, Cambridge, UK). Then, intracellular ROS accumulation was measured by incubating the cells with DCFH-DA fluorescent dye and observing via fluorescence microscopy (Olympus, Tokyo, Japan) (20 $\times$  magnification). The images shown are representative of three experiments. Data are expressed as the mean  $\pm$  SEM ( $n=6$ ). \* $p < 0.05$  compared with the control group. ### $p < 0.001$  compared with the LPS-treated group. Scale bar: 200  $\mu\text{m}$ .

tracellular ROS formation to 127.0% compared with controls ( $p<0.05$ ) (Fig. 4A). However, 7,3',4'-THIF (10, 25, and 50  $\mu\text{M}$ ) markedly reduced this increased ROS production to 52.8%, 46.5%, and 39.7% of the control values, respectively, in a concentration-dependent manner ( $p<0.05$ ,  $p<0.05$ , and  $p<0.05$ , respectively) (Fig. 4A). Additionally, fluorescence microphotographs of cells stained with DCFH-DA showed increased intensity of ROS fluorescence following LPS stimulation; this effect was decreased by treatment with 7,3',4'-THIF (Fig. 4B). These results demonstrate that 7,3',4'-THIF pretreatment inhibits LPS-induced ROS production in BV2 microglial cells.

### Effects of 7,3',4'-THIF on LPS-induced phosphorylation of ERK, JNK, Akt, and GSK-3 $\beta$ and activation of NF- $\kappa\text{B}$ in BV2 microglial cells

To further understand mechanisms underlying the action of 7,3',4'-THIF, we examined the expression levels of ERK and JNK using western blotting. In the presence of LPS, the phosphorylation levels of ERK and JNK increased to 170.9% ( $p<0.01$ ) (Fig. 5A) and 1126.0% ( $p<0.001$ ) (Fig. 5B) of the control values, respectively. However, 25  $\mu\text{M}$  7,3',4'-THIF significantly inhibited the expression of phosphorylated ERK to 68.5% of the LPS-treated group ( $p<0.01$ ) (Fig. 5A). Treatment with 50  $\mu\text{M}$  7,3',4'-THIF significantly suppressed the phosphorylation levels of ERK and JNK to 58.2% ( $p<0.01$ ) (Fig. 5A) and 47.3% ( $p<0.01$ ) (Fig. 5B) of the LPS-treated values,

respectively. Furthermore, LPS treatment of microglia significantly increased Akt and GSK-3 $\beta$  phosphorylation to 181.9% ( $p<0.01$ ) (Fig. 5C) and 140.2% ( $p<0.001$ ) (Fig. 5D) of the control values, respectively. Upon pretreatment with 50  $\mu\text{M}$  7,3',4'-THIF, Akt phosphorylation remained unchanged but the elevated GSK phosphorylation was significantly downregulated to 68.3% of the LPS-treated value ( $p<0.05$ ) (Fig. 5C, 5D).

Finally, we investigated the expression levels of NF- $\kappa\text{B}$ , a crucial transcription factor that modulates neuroinflammatory responses in microglia. LPS significantly increased NF- $\kappa\text{B}$  expression to 189.4% of the control values ( $p<0.05$ ) (Fig. 5E). However, 50  $\mu\text{M}$  7,3',4'-THIF suppressed this NF- $\kappa\text{B}$  expression to 86.48% of the control values ( $p<0.05$ ) (Fig. 5E).

## DISCUSSION

The daidzein metabolite 7,3',4'-THIF possesses potential pharmacological activities. Owing to its antioxidant, antipollutant, and anti-amnesic effects, 7,3',4'-THIF may be a novel candidate for pharmaceutical applications (Huang *et al.*, 2018; Kim *et al.*, 2020; Park *et al.*, 2020). Another major metabolite of daidzein 7,8,4'-THIF exerts strong antineuroinflammatory effects against LPS-induced neurotoxicity through activation of the NF- $\kappa\text{B}$  signaling pathway and inhibition of COX-2 activity in BV2 microglial cells (Wu *et al.*, 2018). We therefore ex-

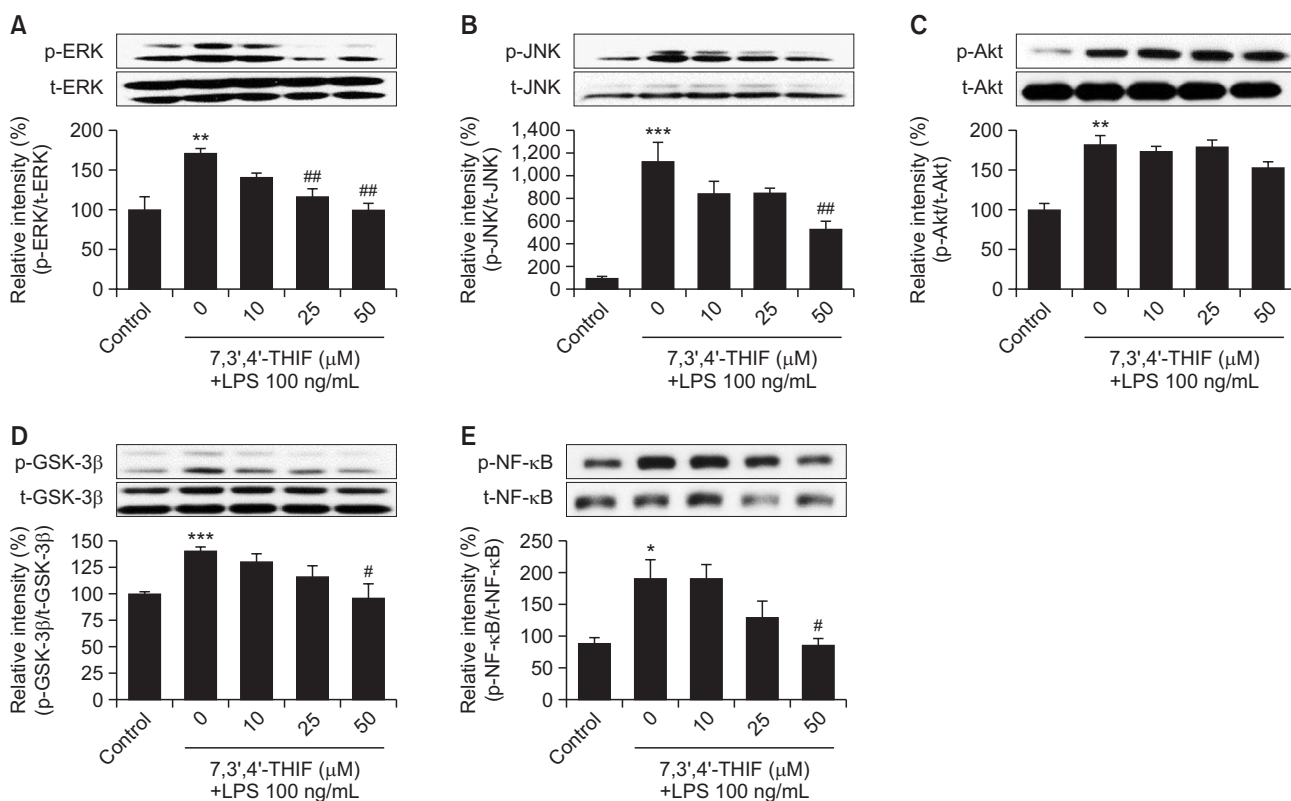


**Fig. 5.** Effects of 7,3',4'-THIF on LPS-induced phosphorylation of ERK 1/2 (A), JNK (B), Akt (C), GSK-3 $\beta$  (D), and NF- $\kappa\text{B}$  (E) in BV2 microglial cells. Cells were pretreated with the indicated concentrations of 7,3',4'-THIF (10, 25, or 50  $\mu\text{M}$ ) for 30 min and then activated with 100 ng/mL LPS for 1 h. Expression levels of p-ERK 1/2, p-JNK, p-Akt, p-GSK-3 $\beta$ , and p-NF- $\kappa\text{B}$  were determined by western blotting. Densitometric results are expressed as the mean  $\pm$  SEM ( $n=3-4$ ). \* $p<0.05$ , \*\* $p<0.01$ , and \*\*\* $p<0.001$  compared with the control group. # $p<0.05$  and ## $p<0.01$  compared with the LPS-treated group.

pected 7,3',4'-THIF to exert protective effects against inflammation-induced neurotoxicity. Recent evidence suggests that the inhibition of neuroinflammatory responses is an important therapeutic strategy for neurodegenerative disorders such as AD and PD. The present study showed that 7,3',4'-THIF treatment mitigated LPS-induced neurotoxicity; inflammatory responses; ROS production; and MAPK, GSK-3 $\beta$ , and NF- $\kappa$ B signaling activation in BV2 microglia.

Microglial activation is an important feature of neurodegenerative disorders including AD. Therefore, we assessed the effect of 7,3',4'-THIF on neuroinflammation using LPS-stimulated BV2 microglial cells in the present study. Activated microglia increases the levels of proinflammatory cytokines IL-6, IL-1 $\beta$ , and TNF- $\alpha$  (Lull and Block, 2010). These mediators contribute to neuronal cell injury and eventually trigger inflammatory cascades (Hemmer *et al.*, 2001). Proinflammatory cytokines are markedly elevated in AD patients (Kaur *et al.*, 2019). Moreover, other important mediators of inflammatory responses such as iNOS and COX-2 may induce neuronal death and promote neurodegeneration (Dulla *et al.*, 2016). Our results showed that NO release induced by LPS, a representative inflammation-inducing agent, was inhibited by both pre- and posttreatment with 7,3',4'-THIF in BV2 microglial cells. To assess whether these effects were curative or preventive, the NO assay was applied before and after the treatment of LPS-stimulated microglia with 7,3',4'-THIF. We observed that 7,3',4'-THIF treatment significantly suppressed LPS-induced iNOS and COX-2 expression and proinflammatory cytokine levels. Thus, 7,3',4'-THIF ameliorated inflammatory responses in microglial and may therefore serve as a therapeutic resource in the prevention or/and treatment of neurodegenerative disorders.

Evidence indicates that elevated ROS levels are associated with neurodegenerative disorders such as AD (Block *et al.*, 2007). Previous studies have demonstrated that microglia activation is an important factor for ROS generation, and excess ROS production in microglial cells is closely linked to brain damage resulting from high proinflammatory mediator or cytokine levels (Floyd and Hensley, 2002). Furthermore, ROS trigger inflammatory cascades through activation of the MAPK, PI3K/Akt, and GSK-3 $\beta$  signaling pathways (Salminen *et al.*, 2008; Hsieh *et al.*, 2010). These signaling cascades further activate NF- $\kappa$ B and its subsequent inflammatory molecules in microglia (Gao *et al.*, 2019; Huang *et al.*, 2019). Therefore, decreasing ROS production in microglia may be an effective strategy for protecting against inflammatory damage. In this study, while LPS treatment significantly increased ROS production, 7,3',4'-THIF pretreatment significantly decreased LPS-induced ROS generation in BV2 microglial cells. Thus, 7,3',4'-THIF may decrease LPS-induced aberrant production of proinflammatory factors such as NO in microglia by inhibiting ROS generation.

Several results suggest that the MAPK, PI3K/Akt, GSK-3 $\beta$ , and NF- $\kappa$ B signaling cascades mediate inflammatory processes. Previous studies on microglia have shown that phosphorylated MAPK, PI3K/Akt, and GSK-3 $\beta$  activate NF- $\kappa$ B, leading to elevated expression of inflammatory mediators such as iNOS, COX-2, and proinflammatory cytokines (Surh *et al.*, 2001; Yuskaitis and Jope, 2009). Therefore, these mediators play crucial roles in inflammatory processes in microglial cells and may serve as therapeutic targets for neuroinflammation-related symptoms. Furthermore, NF- $\kappa$ B activation in microglia con-

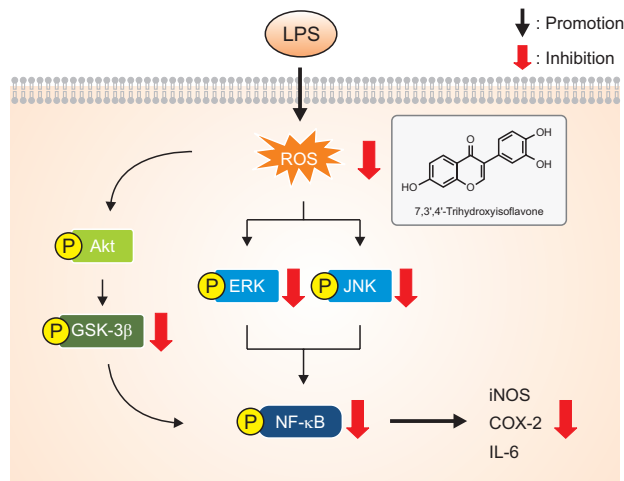


**Fig. 6.** Proposed schematic of the molecular mechanisms of the effects of 7,3',4'-THIF on LPS-induced neuroinflammation in BV2 microglial cells. LPS induces phosphorylation of MAPK signaling molecules (JNK and ERK 1/2) as well as GSK-3 $\beta$  and NF- $\kappa$ B. This activation of NF- $\kappa$ B induces expression of its target genes such as iNOS and COX-2, resulting in the production of NO and pro-inflammatory cytokines such as IL-6, and in the accumulation of ROS. Release of these inflammatory mediators leads to neuroinflammation and neuronal cell injury. Pretreatment of BV2 microglial cells with 7,3',4'-THIF inhibits LPS-induced inflammatory responses through inhibition of MAPK signaling molecules and GSK-3 $\beta$  and NF- $\kappa$ B.

tributes to neuronal damage and neurodegeneration (Mattson, 2005). In addition, NF- $\kappa$ B—a central mediator of inflammatory responses—can be stimulated by various inflammatory factors such as LPS and cytokines (O'Neill and Kaltschmidt, 1997). Therefore, in this study, we performed western blotting to elucidate the effects of 7,3',4'-THIF on LPS-induced MAPK, PI3K/Akt, and GSK-3 $\beta$ , and NF- $\kappa$ B signaling in BV2 microglial cells. Our results showed that while LPS treatment significantly increased phosphorylation of MAPK, Akt, GSK-3 $\beta$ , and NF- $\kappa$ B in BV2 microglial cells, 7,3',4'-THIF effectively inhibited this effect, except in Akt. These findings suggested that the 7,3',4'-THIF-mediated inhibition of inflammatory factors may result, at least in part, from the blockade of MAPK, GSK-3 $\beta$ , and NF- $\kappa$ B activation.

In conclusion, as depicted in Fig. 6, 7,3',4'-THIF, a major daidzein metabolite, effectively protected BV2 microglial cells against LPS-induced neurotoxicity, oxidative stress, and inflammatory responses. These beneficial effects may result from the inhibition of NO release and reduction of iNOS, COX-2, and proinflammatory cytokine levels. In addition, 7,3',4'-THIF significantly suppressed LPS-induced ROS production. The antineuroinflammatory effects of 7,3',4'-THIF may result from the inhibition of MAPK and NF- $\kappa$ B signaling pathways. Further studies are warranted to investigate whether 7,3',4'-THIF protects against inflammation-induced neuronal injury in animal models. 7,3',4'-THIF may be a promising approach for the treatment of inflammation-related neurodegenerative disorders.

## CONFLICT OF INTEREST

The authors have no conflicts of interest to declare.

## ACKNOWLEDGMENTS

This work was supported by a grant (NRF-2017R1A2B 2002428) from the Basic Science Research Program through the National Research Foundation of South Korea.

## REFERENCES

- Block, M. L., Zecca, L. and Hong, J. S. (2007) Microglia-mediated neurotoxicity: uncovering the molecular mechanisms. *Nat. Rev. Neurosci.* **8**, 57-69.
- Chang, T. S. (2014) Isolation, bioactivity, and production of ortho-hydroxydaidzein and ortho-hydroxygenistein. *Int. J. Mol. Sci.* **15**, 5699-5716.
- Cui, Y., Park, J. Y., Wu, J., Lee, J. H., Yang, Y. S., Kang, M. S., Jung, S. C., Park, J. M., Yoo, E. S., Kim, S. H., Ahn Jo, S., Suk, K. and Eun, S. Y. (2015) Dieckol attenuates microglia-mediated neuronal cell death via ERK, Akt and NADPH oxidase-mediated pathways. *Korean J. Physiol. Pharmacol.* **19**, 219-228.
- Dulla, Y. A., Kurauchi, Y., Hisatsune, A., Seki, T., Shudo, K. and Katsuki, H. (2016) Regulatory mechanisms of vitamin D3 on production of nitric oxide and pro-inflammatory cytokines in microglial BV-2 cells. *Neurochem. Res.* **41**, 2848-2858.
- Floyd, R. A. and Hensley, K. (2002) Oxidative stress in brain aging. Implications for therapeutics of neurodegenerative diseases. *Neurobiol. Aging* **23**, 795-807.
- Gao, L., Han, H., Wang, H., Cao, L. and Feng, W. H. (2019) IL-10 knockdown with siRNA enhances the efficacy of Doxorubicin chemotherapy in EBV-positive tumors by inducing lytic cycle via PI3K/p38 MAPK/NF- $\kappa$ B pathway. *Cancer Lett.* **462**, 12-22.
- Hemmer, K., Fransen, L., Vanderstichele, H., Vanmechelen, E. and Heuschling, P. (2001) An *in vitro* model for the study of microglia-induced neurodegeneration: involvement of nitric oxide and tumor necrosis factor- $\alpha$ . *Neurochem. Int.* **38**, 557-565.
- Henn, A., Lund, S., Hedtjarn, M., Schratzenholz, A., Porzgen, P. and Leist, M. (2009) The suitability of BV2 cells as alternative model system for primary microglia cultures or for animal experiments examining brain inflammation. *ALTEX* **26**, 83-94.
- Hsieh, H. L., Wang, H. H., Wu, W. B., Chu, P. J. and Yang, C. M. (2010) Transforming growth factor- $\beta$ 1 induces matrix metalloproteinase-9 and cell migration in astrocytes: roles of ROS-dependent ERK- and JNK-NF- $\kappa$ B pathways. *J. Neuroinflammation* **7**, 88.
- Huang, P. H., Tseng, C. H., Lin, C. Y., Lee, C. W. and Yen, F. L. (2018) Preparation, characterizations and anti-pollutant activity of 7,3',4'-trihydroxyisoflavone nanoparticles in particulate matter-induced HaCaT keratinocytes. *Int. J. Nanomedicine* **13**, 3279-3293.
- Huang, X., Xi, Y., Mao, Z., Chu, X., Zhang, R., Ma, X., Ni, B., Cheng, H. and You, H. (2019) Vanillic acid attenuates cartilage degeneration by regulating the MAPK and PI3K/AKT/NF- $\kappa$ B pathways. *Eur. J. Pharmacol.* **859**, 172481.
- Kang, C. H., Jayasooriya, R. G., Choi, Y. H., Moon, S. K., Kim, W. J. and Kim, G. Y. (2013)  $\beta$ -ionone attenuates LPS-induced pro-inflammatory mediators such as NO, PGE2 and TNF- $\alpha$  in BV2 microglial cells via suppression of the NF- $\kappa$ B and MAPK pathway. *Toxicol. In Vitro* **27**, 782-787.
- Kaur, D., Sharma, V. and Deshmukh, R. (2019) Activation of microglia and astrocytes: a roadway to neuroinflammation and Alzheimer's disease. *Inflammopharmacology* **27**, 663-677.
- Kim, S., Lee, M. S., Lee, B., Gwon, W. G., Joung, E. J., Yoon, N. Y. and Kim, H. R. (2014) Anti-inflammatory effects of sargachromenol-rich ethanolic extract of *Myagropsis myagroides* on lipopolysaccharide-stimulated BV-2 cells. *BMC complement. Altern. Med.* **14**, 231.
- Kim, S. K., Ko, Y. H., Lee, S. Y. and Jang, C. G. (2020) Memory-enhancing effects of 7,3',4'-trihydroxyisoflavone by regulation of cholinergic function and BDNF signaling pathway in mice. *Food Chem. Toxicol.* **137**, 111160.
- Klus, K. and Barz, W. (1995) Formation of polyhydroxylated isoflavones from the soybean seed isoflavones daidzein and glycitein by bacteria isolated from tempe. *Arch. Microbiol.* **164**, 428-434.
- Ko, Y. H., Kim, S. K., Kwon, S. H., Seo, J. Y., Lee, B. R., Kim, Y. J., Hur, K. H., Kim, S. Y., Lee, S. Y. and Jang, C. G. (2019a) 7,8,4'-Trihydroxyisoflavone, a metabolized product of daidzein, attenuates 6-hydroxydopamine-induced neurotoxicity in SH-SY5Y Cells. *Biomol. Ther. (Seoul)* **27**, 363-372.
- Ko, Y. H., Kim, S. Y., Lee, S. Y. and Jang, C. G. (2018) 6,7,4'-Trihydroxyisoflavone, a major metabolite of daidzein, improves learning and memory via the cholinergic system and the p-CREB/BDNF signaling pathway in mice. *Eur. J. Pharmacol.* **826**, 140-147.
- Ko, Y. H., Kwon, S. H., Kim, S. K., Lee, B. R., Hur, K. H., Kim, Y. J., Kim, S. E., Lee, S. Y. and Jang, C. G. (2019b) Protective effects of 6,7,4'-trihydroxyisoflavone, a major metabolite of daidzein, on 6-hydroxydopamine-induced neuronal cell death in SH-SY5Y human neuroblastoma cells. *Arch. Pharm. Res.* **42**, 1081-1091.
- Kulling, S. E., Honig, D. M. and Metzler, M. (2001) Oxidative metabolism of the soy isoflavones daidzein and genistein in humans *in vitro* and *in vivo*. *J. Agric. Food Chem.* **49**, 3024-3033.
- Lammersfeld, C. A., King, J., Walker, S., Vashi, P. G., Grutsch, J. F., Lis, C. G. and Gupta, D. (2009) Prevalence, sources, and predictors of soy consumption in breast cancer. *Nutr. J.* **8**, 2.
- Li, N., Liu, B. W., Ren, W. Z., Liu, J. X., Li, S. N., Fu, S. P., Zeng, Y. L., Xu, S. Y., Yan, X., Gao, Y. J., Liu, D. F. and Wang, W. (2016) GLP-2 attenuates LPS-induced inflammation in BV-2 cells by inhibiting ERK1/2, JNK1/2 and NF- $\kappa$ B signaling pathways. *Int. J. Mol. Sci.* **17**, 190.
- Lim, T. G., Lee, S. Y., Duan, Z., Lee, M. H., Chen, H., Liu, F., Liu, K., Jung, S. K., Kim, D. J., Bode, A. M., Lee, K. W. and Dong, Z. (2017) The prolyl isomerase Pin1 is a novel target of 6,7,4'-trihydroxyisoflavone for suppressing esophageal cancer growth. *Cancer Prev. Res. (Phila.)* **10**, 308-318.
- Lu, Y., An, Y., Lv, C., Ma, W., Xi, Y. and Xiao, R. (2018) Dietary soybean isoflavones in Alzheimer's disease prevention. *Asia Pac. J. Clin. Nutr.* **27**, 946-954.
- Lull, M. E. and Block, M. L. (2010) Microglial activation and chronic neurodegeneration. *Neurotherapeutics* **7**, 354-365.
- Mattson, M. P. (2005) NF- $\kappa$ B in the survival and plasticity of neurons. *Neurochem. Res.* **30**, 883-893.
- Miguez, A. C., Francisco, J. C., Barberato, S. H., Simeoni, R., Precoma, D., Do Amaral, V. F., Rodrigues, E., Olandoski, M., de Noronha, L., Greca, F. H., de Carvalho, K. A., Faria-Neto, J. R. and Guarita-Souza, L. C. (2012) The functional effect of soybean extract and isolated isoflavone on myocardial infarction and ventricular dysfunction: the soybean extract on myocardial infarction. *J. Nutr. Biochem.* **23**, 1740-1748.
- O'Neill, L. A. and Kaltschmidt, C. (1997) NF- $\kappa$ B: a crucial transcription factor for glial and neuronal cell function. *Trends Neurosci.* **20**, 252-258.
- Pandur, E., Varga, E., Tamasi, K., Pap, R., Nagy, J. and Sipos, K. (2018) Effect of inflammatory mediators lipopolysaccharide and lipoteichoic acid on iron metabolism of differentiated SH-SY5Y cells alters in the presence of BV-2 microglia. *Int. J. Mol. Sci.* **20**, 17.
- Park, J., Min, J. S., Kim, B., Chae, U. B., Yun, J. W., Choi, M. S., Kong, I. K., Chang, K. T. and Lee, D. S. (2015) Mitochondrial ROS govern the LPS-induced pro-inflammatory response in microglia cells by regulating MAPK and NF- $\kappa$ B pathways. *Neurosci. Lett.* **584**, 191-196.
- Park, S. H., Lee, C. H., Lee, J. Y., Yang, H., Kim, J. H., Park, J. H. Y., Kim, J. E. and Lee, K. W. (2020) Topical application of 7,3',4'-trihydroxyisoflavone alleviates atopic dermatitis-like symptoms in NC/Nga mice. *Planta Med.* **86**, 190-197.
- Roh, C. (2014) Microbial transformation of bioactive compounds and production of ortho-dihydroxyisoflavones and glycitein from natural fermented soybean paste. *Biomolecules* **4**, 1093-1101.
- Rufer, C. E. and Kulling, S. E. (2006) Antioxidant activity of isoflavones and their major metabolites using different *in vitro* assays. *J. Agric. Food Chem.* **54**, 2926-2931.
- Salminen, A., Huuskonen, J., Ojala, J., Kauppinen, A., Kaarniranta,

- K. and Suuronen, T. (2008) Activation of innate immunity system during aging: NF- $\kappa$ B signaling is the molecular culprit of inflamm-aging. *Ageing Res. Rev.* **7**, 83-105.
- Surh, Y. J., Chun, K. S., Cha, H. H., Han, S. S., Keum, Y. S., Park, K. K. and Lee, S. S. (2001) Molecular mechanisms underlying chemo-preventive activities of anti-inflammatory phytochemicals: down-regulation of COX-2 and iNOS through suppression of NF-kappa B activation. *Mutat. Res.* **480-481**, 243-268.
- Villa, A., Vegeto, E., Poletti, A. and Maggi, A. (2016) Estrogens, neuro-inflammation, and neurodegeneration. *Endocr. Rev.* **37**, 372-402.
- Wu, P. S., Ding, H. Y., Yen, J. H., Chen, S. F., Lee, K. H. and Wu, M. J. (2018) Anti-inflammatory activity of 8-hydroxydaidzein in LPS-stimulated BV2 microglial cells via activation of Nrf2-antioxidant and attenuation of Akt/NF-kappaB-inflammatory signaling pathways, as well as inhibition of COX-2 activity. *J. Agric. Food Chem.* **66**, 5790-5801.
- Yuskaitis, C. J. and Jope, R. S. (2009) Glycogen synthase kinase-3 regulates microglial migration, inflammation, and inflammation-induced neurotoxicity. *Cell. Signal.* **21**, 264-273.